Available online at www.sciencedirect.com

ScienceDirect

www.elsevier.com/locate/jes

JES JOURNAL OF ENVIRONMENTAL SCIENCES

www.jesc.ac.cn

Research Article

Multi-endpoint assays reveal more severe toxicity induced by chloraminated effluent organic matter than chloraminated natural organic matter

Hai-Yan Wang[1], *De-Xiu Wu*[2,*], *Ye Du*[3], *Xiao-Tong Lv*[2], *Qian-Yuan Wu*[2]

[1] *State Key Laboratory of Environmental Criteria and Risk Assessment, Chinese Research Academy of Environmental Sciences, Beijing 100012, China*

[2] *Environmental Protection Key Laboratory of Microorganism Application and Risk Control, Guangdong Provincial Engineering Research Center for Urban Water Recycling and Environmental Safety, Tsinghua Shenzhen International Graduate School, Tsinghua University, Shenzhen 518055, China*

[3] *College of Architecture and Environment, Sichuan University, Chengdu 610000, China*

ARTICLE INFO

Article history:
Received 24 October 2022
Revised 7 January 2023
Accepted 8 January 2023
Available online 13 January 2023

Keywords:
Cytotoxicity
Intracellular active nitrogen/oxygen
Intracellular oxidative damage
Cell necrosis
Reclaimed water

ABSTRACT

Disinfection by chloramination produces toxic byproducts and the difference in toxicity of reclaimed and drinking water treated by chloramination remains unclear. This study investigated cytotoxic effects at the same concentrations of dissolved organic matter and showed that chloraminated effluent organic matter (EfOM) induced 1.7 times higher cytotoxicity than chloraminated natural organic matter (NOM) applied to simulate drinking water. Chloraminated EfOM induced more reactive nitrogen species than chloraminated NOM, and chloraminated EfOM and NOM induced similar and higher levels of reactive oxygen species than the negative control, respectively. Consequently, intracellular macromolecule damage indicated by DNA/RNA damage marker 8–hydroxy-(deoxy)guanosine and the intracellular protein carbonyl concentration induced by chloraminated EfOM was higher and slightly more than that induced by chloraminated NOM, respectively. These data were consistent with the effects on cell physiological processes. Cell cycle arrest mainly occurred in G2 phase by chloraminated EfOM and NOM. Early apoptotic cells, which could return to normal, increased upon exposure to high concentrations of chloraminated EfOM and NOM. Moreover, necrotic cells were significantly increased from 0.5% to 2.5% when the concentration increased from 20- to 60-fold chloraminated EfOM, but were not obviously changed by chloraminated NOM. These results indicated that the comprehensive intracellular changes induced by toxic substances in chloraminated EfOM were more irreversible and induced more cell death than chloraminated NOM.

* Corresponding author.
E-mail: dexiu_wu20@163.com (D.-X. Wu).

https://doi.org/10.1016/j.jes.2023.01.009
1001-0742/

Introduction

Reclaimed water is a suitable water resource to replenish surface water where urban rivers and lakes lack natural water supplementation (Sun et al., 2022; Zheng et al., 2022). When supplied and mixed with surface water, there is potential toxicity of disinfected reclaimed water for not only aquatic life, but also humans (Nixdorff et al., 2021; Wang et al., 2021a). Chloramination was commonly used in drinking water and reclaimed water disinfection (Hua and Reckhow, 2007; Jacangelo and Trussell, 2002; Richardson et al., 2008). Besides, during non-nitrified wastewater chlorination, the ammonia in wastewater would react with chlorine to form chloramine (Peng et al., 2022; Schreiber and Mitch, 2006). Monochloramine is the main chloramine species generated during chloramination, which has a strong ability to penetrate biofilms and inactivate micro-biomasses (Lee et al., 2011b). Chloramination results in low concentrations of trihalomethanes (THMs), haloacetic acids (HAAs), and other regulated disinfection byproducts (DBPs) as well as total organic halogen (Krasner et al., 2006; Richardson et al., 2008).

The main concern of a disinfection process is whether the disinfected water is toxic to humans and the ecology. A previous study has reported the toxicity of single DBPs. Haloacetonitriles (HANs) were more toxic than HAAs and halonitromethanes in Chinese hamster ovary (CHO) cells. Haloacetonitriles should be considered carefully during disinfection processes because of their correlation with high toxicity of chlorinated water (Allen et al., 2022; Muellner et al., 2007). Moreover, halophenols are more toxic than THMs and HAAs in terms of developmental toxicity in marine polychaete *Platynereis dumerilii* and autotrophic marine alga *Tetraselmis marina* (Liu and Zhang, 2014; Yang and Zhang, 2013). These findings indicate that HANs and halophenols are much more toxic than THMs and HAAs. However, these data on single DBP toxicity provide a limited overview of water because the mixture is usually comprehensive.

During chloramination, there is a health risk because effluent organic matter (EfOM) in reclaimed water and natural organic matter (NOM) in drinking water form toxic DBPs containing nitrogen. Moreover, despite forming less DBPs, chloramination produces unique DBPs such as cyanogen chloride that is preferentially produced in chloraminated water compared with other disinfection technologies (Krasner et al., 1989). Furthermore, iodinated THMs and dichloroacetaldehyde are more highly produced by chloramination than other disinfection processes (Krasner et al., 2006). Additionally, although nitrogen-containing DBPs are toxic, their concentration is relatively low during disinfection processes (Shah and Mitch, 2012). More importantly, in the presence of monochloramine, halophenols such as 4-iodophenol convert into a higher halogen substitute state including 2,4,6-triiodophenol and 2,6-diiodo-4-nitrophenol (Gong et al., 2017). Decarboxylation and aldehyde pathways of forming nitriles operate simultaneously during chloramination. Nitrile nitrogen originates from primary amine constituents of dissolved organic nitrogen (DON) and inorganic chloramines (Yang et al., 2010). It is very likely that EfOM contains more DON than NOM originating from drinking water, which produces more nitriles (Hu et al., 2016). Additionally, N-nitrosodimethylamine (NDMA) is a byproduct of $NHCl_2$ and amine (e.g., dimethylamine) through nucleophilic substitution and oxidation (Schreiber and Mitch, 2006). Because of the high concentration of amine precursors, the risk of NDMA generated by chloramination in wastewater is high. Therefore, the different DON contents in EfOM and NOM are possibly forming different DBPs and cause potential toxicity in the environment.

Toxicity evaluation of water provides essential information about cell damage and nucleus-level impairment. Disinfected water has been reported to be genotoxic. Genotoxicity including DNA double-strand breaks are induced by chlorinated second effluent, which are among the most dangerous lesions that can occur in the genome of eukaryotic cells (Bassing and Alt 2004; Du et al., 2020). Additionally, the cytotoxicity of halogenated amino acids, halogenated peptides, treated reclaimed water and chlorinated EfOM induce intracellular reactive oxygen species (ROS), revealing oxidative stress as a major toxicity induction pathway (Deng et al., 2022; Du et al., 2020; Tian et al., 2020). Intracellular reactive nitrogen species (RNS) are another major factor in the cell reaction to toxicants. Amino acids and biogenic amines are endogenous nitrogenous compounds in which an electronegative nitrogen atom has an active lone pair of electrons. They are vulnerable N-nucleophiles and can be attacked by exogenous substances or metabolites produced from furans, naphthalene, benzene, and products of lipid peroxidation (Zhang et al., 2021b). Thus, the development, metabolism, and physiological functions of organisms (e.g., intracellular replication, transcription, translation, division and proliferation, DNA and protein synthesis, apoptosis regulation, and intercellular communication) are disrupted. Previous studies have reported toxicity changes and toxicant formation in water treated by chlorination, ozonation, and chloramination (Nobukawa and Sanukida 2000; Wang et al., 2021b; Zhang et al., 2021a). Understanding the possible toxification pathways is necessary to control toxicity. Compared with chlorination that has characterized toxification mechanisms (Du et al., 2020), the toxification pathways and mechanisms of chloraminated NOM and EfOM are unclear.

Therefore, to understand the difference in toxicity induced by chloraminated EfOM and NOM, we investigated changes in intracellular substances including reactive species and oxidative damage to macromolecules. Then, we focused on cell physiological processes and cytotoxicity. As a result, the toxification pathways and mechanism of cytotoxicity corresponding to changes in intracellular substances were revealed.

1. Materials and methods

1.1. *Water sampling and analysis*

Reclaimed water was collected from a clarifier after biological treatment by an anaerobic-anoxic-oxic (A^2O) process at a municipal sewage treatment plant in Shenzhen, China. Reclaimed water samples were filtered through 0.45 μm cellulose acetate membranes and then stored at 2–4°C. The standard of Suwannee River natural organic matter (2R1N1, 50.7% carbon content) was purchased from the International Humus Substances Society. NOM was dissolved in ultrapure water and

diluted to the same DOC concentration (5 mg C/L, pH=7) as the reclaimed water used in the same experiment.

1.2. *Chloramination*

Chloramine disinfectant was prepared with sodium hypochlorite and ammonium chloride. In accordance with the concentration of the sodium hypochlorite stock solution, a chloramine solution was prepared at a molar ratio of NaClO:NH_4Cl= 0.8:1 (the Cl/N mass ratio is 2). The NaClO solution was added to an NH_4Cl solution and mixed quickly. Absorbance of the prepared chloramine solution was recorded at 245 and 295 nm. When the absorbance at 245 nm was much higher than that at 295 nm, the monochloramine concentration in the solution was much higher than that of dichloramine, and a disinfectant mainly composed of monochloramine was obtained. The role of dichloramine and trichloramine generated under higher Cl/N mass ratio is suggested to study in the future and the reactions were shown in Appendix A Text S1. The total chlorine concentration was measured by a residual chlorine analyzer (Hach, DR3900). After chloramination for 1 hr, the residual oxidant was quenched by a 1.05 stoichiometric amount of ascorbic acid.

1.3. *Toxicity analysis*

Reclaimed water samples and NOM solutions after chloramination were concentrated by solid phase extraction as reported previously (Yang et al., 2021). In brief, after adjusting the pH to 2 with 4 mol/L HCl, samples were passed through HLB cartridges (Oasis, Waters, Milford, MA, USA) at 4 mL/min. Cartridges were dried with pure nitrogen gas and then eluted with methanol, acetone, and dichloromethane. Then, nitrogen gas was used to dry the organic solution that was redissolved in DMEM/F-12 medium (1:1) (Cytiva) with 0.5% dimethyl sulfoxide.

CHO cells (American Type Culture Collection) at passage 2–4 was collected, seeded at 10,000 cells per well in 96-well plates, and treated with a gradient of diluted water samples. Intracellular RNS and ROS, base oxidated modification product 8–hydroxy-(deoxy)guanosine [8-OH(d)G], and the cell cycle were analyzed by a high content analysis system (ImageXpress® Micro, Molecular Devices, USA) as reported previously (Du et al., 2020; Wu et al., 2019; Yang et al., 2021). RNS and ROS were measured by an intracellular total RNS and ROS assay kit (STA-800, Oxiselect™; KA4075, Abnova). The 8-OH(d)G assay was performed by fixation, immunofluorescence staining, and fluorescence intensity measurement using the high content analysis system. The cell cycle was analyzed by the fluorescence intensity of DNA stained with propidium iodide. Protein carbonyl was measured using an OxiSelect™ protein carbonyl ELISA kit (Cell Biolabs) by recording absorbance at 450 nm in a SpectraMax i3 (Molecular Devices, USA). Apoptosis and necrosis were evaluated by flow cytometry (FACSCalibur, BD, USA) using an Annexin V/PI cell apoptosis kit (BD Pharmingen) (Du et al., 2020). Each water sample was analyzed in triplicate. The toxicity assay advantages and disadvantages were listed in Appendix A Table S1.

Cell viability was quantified by the intracellular adenosine triphosphate (ATP) concentration using a CellTiter-Glo® luminescent cell viability assay kit (Promega) as reported previously (Du et al., 2020). Phenol dissolved in culture medium was used as the positive control to calculate the cytotoxicity equivalent. The cytotoxicity equivalent was calculated as the LC_{50} of phenol (positive control, LC_{50}=550 mg phenol/L) divided by that of the sample.

1.4. *Statistical analysis*

The Kruskal–Wallis test and one-way analysis of variance were applied to evaluate the significance of differences among samples using Origin 2022 software (academic version). Concentration–effect curves of cytotoxicity were constructed from dose-response curves in Origin 2022 software and the LC_{50} was obtained from the plot.

2. Results and discussion

2.1. *Formation of intracellular reactive species*

Intracellular ROS include hydrogen peroxide and superoxide. RNS include nitric oxide, peroxynitrite, and reactive lipid species. As shown in Fig. 1, intracellular ROS and RNS were produced when cells were exposed to chloraminated organic matter. The ROS relative induction rate of chloraminated EfOM was slightly higher than that of chloraminated NOM. Although chloraminated EfOM had a higher RNS relative induction rate than chloraminated NOM, the RNS induction rate was lower than ROS. Specifically, when the relative RNS induction rate was 150%, the concentration of chloraminated NOM ranged from 60- to 80-fold, whereas that of chloraminated EfOM was more than 20-fold. However, when the relative ROS induction rate was 150%, the concentrations of chloraminated NOM and EfOM were approximately 20-fold. Therefore, ROS were more severe than RNS, ROS induced by chloraminated NOM and EfOM were similar, and RNS were more induced by chloraminated EfOM.

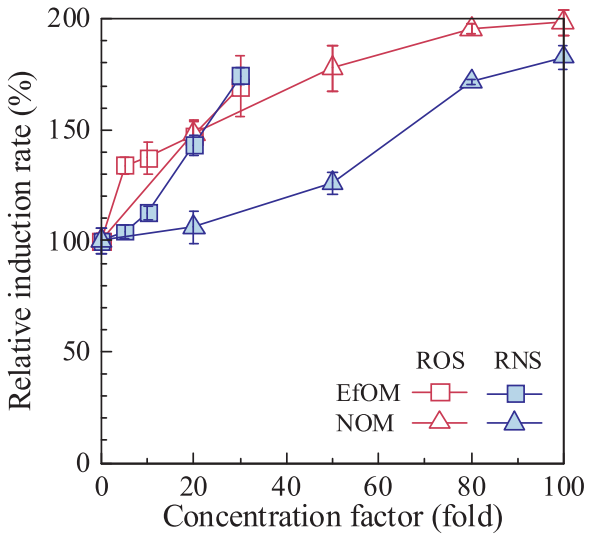

Fig. 1 – The influence on intracellular ROS and RNS by chloraminated EfOM and chloraminated NOM.

Oxidative stress occurs by an imbalance of ROS or RNS generation and the cellular antioxidant capacity (Chiarello et al., 2020). At low levels, ROS and RNS are signaling molecules. However, at high levels, they damage organelles such as mitochondria. Oxidative stress and the associated mitochondrial dysfunction may result in energy depletion, accumulation of cytotoxic mediators, and finally induced cell death (Lee et al., 2011a). Therefore, ROS are essential, but capable of damaging cells in terms of cell physiological processes including cell differentiation, proliferation, the oxidative defense system, and mitogenicity (Chiarello et al., 2020). Intracellular ROS delays mitophagy and results in cell death. It has been suggested that ROS are an important toxicity pathway for dihalogenated compounds that are a group of model DBPs (Brambilla et al., 2020; Girard et al., 2008; Tian et al., 2020). ROS and RNS react and convert to each other. Superoxide and hydrogen peroxide react with nitric oxide to produce peroxynitrite and oxidized lipids to produce reactive lipid species that damage membrane phospholipids (Chiarello et al., 2020; Lee et al., 2011a). Additionally, EfOM contains a higher proportion of DON and low molecular weight compounds than NOM, making EfOM vulnerable to forming more nitrogen-containing reactive compounds that attack cells and even enter cells (Hu et al., 2016). Thus, more intracellular RNS were formed upon exposure to chloraminated EfOM.

2.2. *Damage of intracellular macromolecules*

The lipid order in phospholipid bilayers decreases and pores form when cells are exposed to oxidative substances. And exogenous substances enter the cell causes oxidative damage to cellular macromolecules (Van der Paal et al., 2016). Intracellular macromolecules DNA, RNA, and proteins are easily attacked by reactive species because of their low redox potential groups (Van der Paal et al., 2016; Zhang et al., 2021a). Guanosine is vulnerable to oxidization into hydroxylated products at the C-8 position and form 8-OH(d)G. Lipids are oxidized and convert into reactive lipids that produce protein–protein cross-linkages and carbonyl acid derivatives by oxidizing amino acid residues of proteins (Gobi et al., 2018).

The influence of chloraminated EfOM and NOM on intracellular 8-OH(d)G and protein carbonyl formation is shown in Fig. 2. Chloraminated EfOM was more inductive to form 8-OH(d)G than chloraminated NOM (Fig. 2a). When the induction rate was 120%, the concentration of chloraminated NOM was approximately 60-fold, whereas that of chloraminated EfOM was 20-fold. This not only indicated more severe toxic effects of chloraminated EfOM than chloraminated NOM, but also more severe induction of 8-OH(d)G than intracellular ROS and RNS shown in Fig. 1 because of the lower concentration with the same induction rate. As shown in Fig. 2b, protein carbonyl concentrations under 10–40-fold-concentrated chloraminated EfOM were higher than those with chloraminated NOM. At a 50-fold concentration, formation of protein carbonyl was similar for both chloraminated EfOM and NOM, and both were higher than the negative controls. Although chloraminated NOM resulted in high induction of protein carbonyl at 80- and 100-fold, the cell death ratio increased because of the toxic effect exerted by chloraminated EfOM. Therefore, no data were obtained at 80- and 100-fold concentrations of chloraminated EfOM. Reclaimed water, chlorinated and ozonated effluent, and chlorinated NOM induce 8-OH(d)G in mammalian cells (Du et al., 2020; Wu et al., 2019; Xu et al., 2020). Our study confirmed induction of damage to intracellular macromolecules by chloraminated EfOM and NOM. Because the macromolecules were damaged, corresponding physiological processes, including cell cycle arrest and necrosis, occurred in the cells.

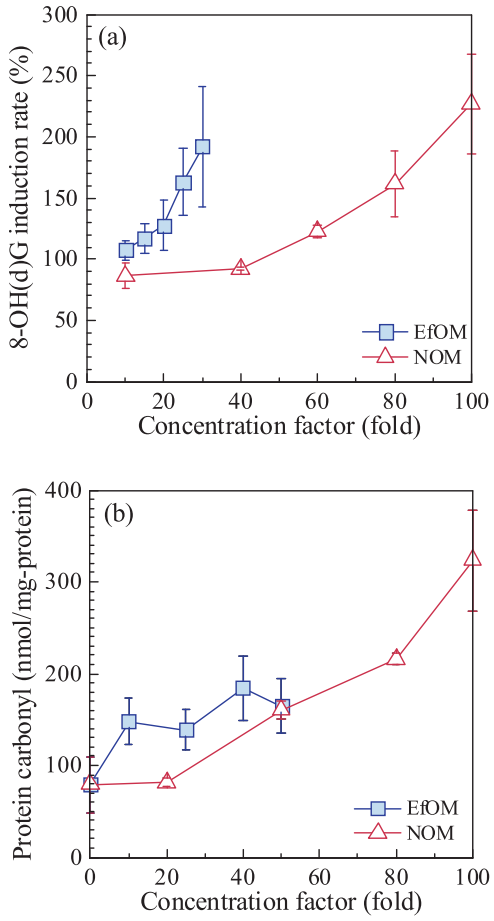

Fig. 2 – The influence on (a) Intracellular DNA/RNA damage 8-OH(d)G and (b) protein carbonyl by chloraminated EfOM and chloraminated NOM.

2.3. *Cell physiological processes*

2.3.1. *Cell cycle arrest*

When DNA is damaged, cell division is blocked by cell cycle arrest to repair the DNA (Shackelford et al., 1999). The cell cycle includes mitosis (M phase) and interphase that has three ordered periods: G_0/G_1 phase for DNA replication material preparation, S phase for DNA replication, and G_2 phase for cell division material preparation.

CHO cell cycles after exposure to the samples for 24 hr are shown in Fig. 3. After treatment with chloraminated EfOM, the proportion of cells in G2 phase was increased when the concentration was increased, indicating that the cell cycle may be blocked in G2 phase. Sixty-fold-concentrated chloraminated EfOM induced a 2.2-fold increase in the proportion of G2 cells

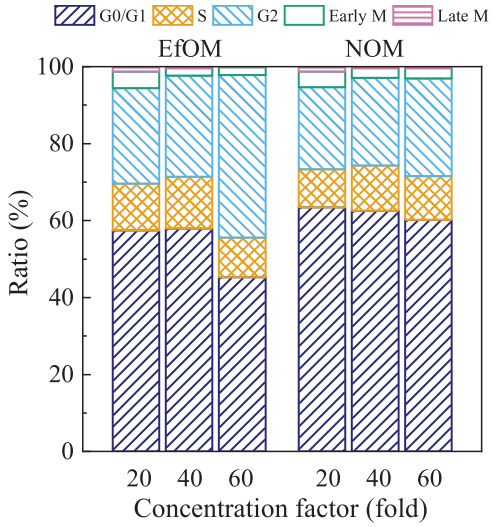

Fig. 3 – Disturbance to CHO cell cycle arrest when exposed to chloraminated EfOM and chloraminated NOM.

(42.2%) compared with the negative control (19.3%). Chloraminated NOM produced similar results, but a lower proportion of cells in G2 phase arrest (25.4%) at a 60-fold concentration. Because the proportion of cells in G2 phase was increased, the proportions of cells in G1 and M phases were decreased correspondingly. These high concentrations caused obvious disturbance of the cell cycle, indicating intracellular damage caused by chloraminated EfOM and NOM. Additionally, chloraminated EfOM caused more severe cell cycle arrest than chloraminated NOM, which was consistent with the results in sections Figs. 1 and 2.

ROS affect signal transduction related to regulation of the cell cycle and results in a temporary block of the cell cycle. Specifically, ROS cause DNA damage and inhibit cyclin-dependent kinases. G1, S, G2, or M phase may be temporarily or permanently blocked, and cells permanently blocked in G2, S, and M phases undergo apoptosis (Boonstra and Post, 2004).

2.3.2. *Cell apoptosis and necrosis*

When DNA damage is repairable in early apoptotic cells, the cells will return to normal. Otherwise, they will undergo irreversible cell death (Luo et al., 2020). As shown in Fig. 4a, cells exposed to high concentrations of water samples showed high early apoptosis, late apoptosis, and necrosis. When the concentration increased from 20- to 60-fold, the proportion of early apoptotic cells increased from 5.8% to 8.7% and from 3.3% to 6.3% when exposed to chloraminated EfOM and NOM,

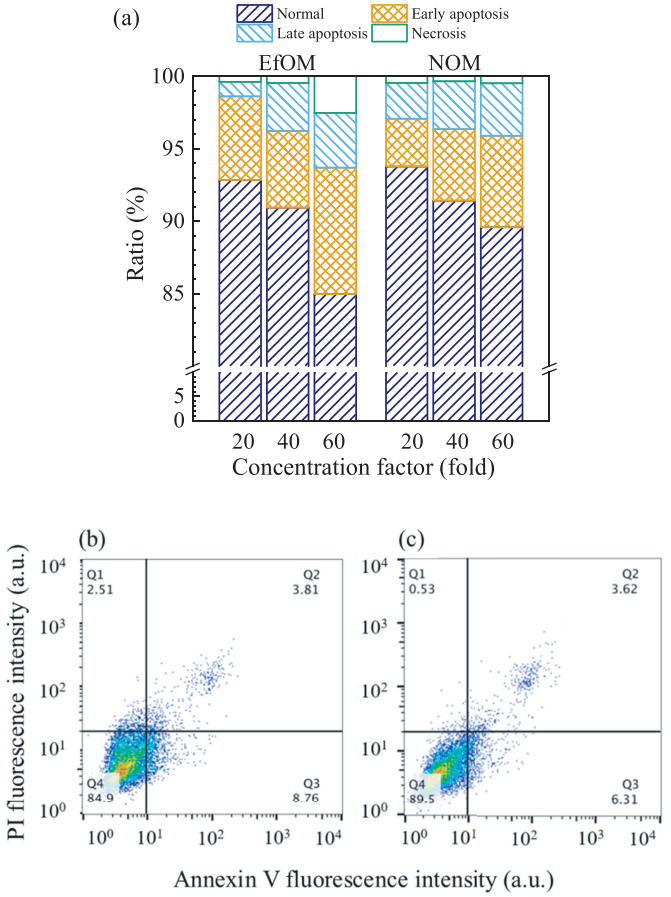

Fig. 4 – Disturbance to CHO cell apoptosis and necrosis when exposed to chloraminated EfOM and chloraminated NOM (a) ratios of cells under 20, 40, 60 folds concentration factors. Annexin V/PI double staining results of (b) reclaimed water and (c) NOM contacted CHO cells for 24 hr before and after chloramination where water samples were concentrated 60 folds. Q1: cells underwent necrosis, Q2: cells underwent late apoptosis, Q3: cells underwent early apoptosis, Q4: normal cells.

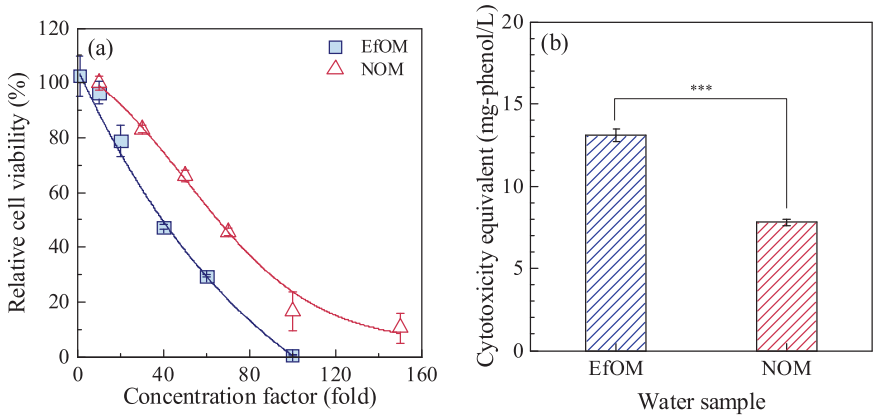

Fig. 5 – Cytotoxicity (a) concentration-effect curves and (b) equivalent induced by chloraminated EfOM and chloraminated NOM. "*" refers to $p < 0.001$.**

respectively. The proportions of cells in late apoptosis induced by 20- and 60-fold-concentrated chloraminated EfOM and NOM increased from 1.0% to 3.8% and 2.5% to 3.6%, respectively. Furthermore, the proportion of necrotic cells caused by chloraminated EfOM was 2.5%, which was significantly higher than that caused by chloraminated NOM at 60-fold ($p < 0.001$). At a 60-fold concentration, cells exposed to chloraminated EfOM showed higher necrosis, late apoptosis, and early apoptosis distributions compared with chloraminated NOM (Fig. 4b and c). Although the overall proportions of cells were normal, the high proportion of cells in early apoptosis induced by chloraminated NOM suggested reversibility upon removal of the toxicants (Elmore, 2007).

2.4. *Cytotoxicity*

Concentration–effect curves of cytotoxicity are shown in Fig. 5a. The concentration–effect curves were clearly separate as CHO cells were exposed to chloraminated EfOM and NOM. As shown in Fig. 5b, the toxicity equivalent caused by chloraminated EfOM was 13.1 mg phenol/L and significantly higher than 7.8 mg phenol/L induced by chloraminated NOM ($p < 0.001$). The higher cytotoxicity caused by chloraminated EfOM was consistent with the more sever effects including more macromolecule damage and disturbance to cell physiological processes caused by more intracellular RNS and ROS. H^+ is essential for ATP synthesis, which is consumed when forming intracellular ROS and RNS, and hinders ATP synthesis (Turrens, 2003). Combined with the results of reactive species in Fig. 1, the accumulation of ROS and RNS in cells caused by water samples may decrease the ATP concentration and reduce cell viability.

The toxic effects on CHO cells can be explained by the possible variance in DBP formation between EfOM and NOM. EfOM generates more total organic halogen and highly toxic nitrogenous DBPs (e.g., dichloroacetonitrile and trichloronitromethane) than NOM during chlorination (Du et al., 2020). Application of ^{15}N-labeled monochloramine figured DBPs including dichloroacetonitrile and dichloroacetamide nitrogen came from organic nitrogen precursors, and inorganic chloramines are also precursors of nitrile (Huang et al., 2012). NDMA also forms as DBPs because of the high concentration of amine precursors in EfOM through a dichloramine nucleophilic substitution reaction (Shah and Mitch, 2012). This can be attributed to EfOM containing a higher proportion of DON than drinking water organic matter. Inorganic nitrogen including ammonia and nitrate convert into DON in wastewater treatment plants (Lin et al., 2021). Furthermore, EfOM exhibits three to five times higher estrogenic activity and at least one times higher genotoxicity than NOM (Hu et al., 2016). Our results highlighted the stronger toxicity of chloraminated EfOM than NOM by inducing more irreversible effects in cells. Therefore, the risks posed by effluent chloramination are suggested to be controlled carefully during reclaimed water disinfection.

3. Conclusion

Chloramination is widely applied in drinking water and wastewater treatment plants. To understand the difference in the potential risks caused by chloramination in wastewater and drinking water, we applied multiple toxicity assays to evaluate cell reactions to chloraminated NOM and EfOM. The main conclusions were as follows:

(1) Intracellular reactive species including ROS and RNS were over generated when cells were exposed to chloraminated EfOM and NOM. ROS formation induced by chloraminated EfOM and NOM was similar, but chloraminated EfOM induced more RNS than chloraminated NOM.
(2) DNA/RNA damage marker 8-OH(d)G was produced after chloraminated EfOM or NOM treatment of cells. The increase in the 8-OH(d)G induction rate in chloraminated EfOM-treated cells was higher than that in cells treated with chloraminated NOM. Cellular macromolecules were damaged as a result of attack by intracellular reactive species.
(3) Cell cycle arrest in G2 phase was broadly observed after exposure to chloraminated EfOM and NOM. The G2 phase arrest caused by chloraminated EfOM was more severe and the corresponding proportion of necrotic cells was also higher compared with chloraminated NOM.

(4) As a comprehensive index, the cytotoxicity induced by chloraminated EfOM was higher than that induced by chloraminated NOM. The probable reason was that the intracellular changes induced by toxic substances in chloraminated EfOM were more irreversible and thus inevitably led to cell death.

Declaration of Competing Interest

The authors declare that they have no known competing financial interests or personal relationships that could have appeared to influence the work reported in this paper.

Acknowledgment

This study was supported by the National Key R&D Program of China (No. 2020YFC1806302), National Natural Science Foundation of China (No. 52022049/51978370), Guangdong Basic and Applied Basic Research Foundation (No. 2020A1515110106).

Appendix A Supplementary data

Supplementary material associated with this article can be found, in the online version, at doi:10.1016/j.jes.2023.01.009.

References

Allen, J.M., Plewa, M.J., Wagner, E.D., Wei, X., Bokenkamp, K., Hur, K., et al., 2022. Drivers of disinfection byproduct cytotoxicity in U.S. drinking water: should other dbps be considered for regulation? Environ. Sci. Technol. 56 (1), 392–402.

Bassing, C.H., Alt, F.W., 2004. The cellular response to general and programmed DNA double strand breaks. DNA Repair 3 (8), 781–796 (Amst.).

Boonstra, J., Post, J.A., 2004. Molecular events associated with reactive oxygen species and cell cycle progression in mammalian cells. Gene 337, 1–13.

Brambilla, L., Lahiri, T., Cammer, M., Levy, D.E., 2020. STAT3 inhibitor OPB-51602 is cytotoxic to tumor cells through inhibition of complex I and ROS induction. iScience 23 (12), 101822.

Chiarello, D.I., Abad, C., Rojas, D., Toledo, F., Vázquez, C.M., Mate, A., et al., 2020. Oxidative stress: normal pregnancy versus preeclampsia. Biochim. Biophys. Acta 1866 (2), 165354.

Deng, Y., Zhang, Y., Ren, H., 2022. Multi-omic studies on the toxicity variations in effluents from different units of reclaimed water treatment. Water Res. 208, 117874.

Du, Y., Wang, W.L., He, T., Sun, Y.X., Lv, X.T., Wu, Q.Y., et al., 2020. Chlorinated effluent organic matter causes higher toxicity than chlorinated natural organic matter by inducing more intracellular reactive oxygen species. Sci. Total Environ. 701, 134881.

Elmore, S., 2007. Apoptosis: a review of programmed cell death. Toxicol. Pathol. 35 (4), 495–516.

Girard, P.M., Pozzebon, M., Delacôte, F., Douki, T., Smirnova, V., Sage, E., 2008. Inhibition of S-phase progression triggered by UVA-induced ROS does not require a functional DNA damage checkpoint response in mammalian cells. DNA Repair 7 (9), 1500–1516 (Amst.).

Gobi, N., Vaseeharan, B., Rekha, R., Vijayakumar, S., Faggio, C., 2018. Bioaccumulation, cytotoxicity and oxidative stress of the acute exposure selenium in Oreochromis mossambicus. Ecotoxicol. Environ. Saf. 162, 147–159.

Gong, T., Tao, Y., Zhang, X., Hu, S., Yin, J., Xian, Q., et al., 2017. Transformation among aromatic iodinated disinfection byproducts in the presence of monochloramine: from monoiodophenol to triiodophenol and diiodonitrophenol. Environ. Sci. Technol. 51 (18), 10562–10571.

Hu, H.Y., Du, Y., Wu, Q.Y., Zhao, X., Tang, X., Chen, Z., 2016. Differences in dissolved organic matter between reclaimed water source and drinking water source. Sci. Total Environ. 551-552, 133–142.

Hua, G., Reckhow, D.A., 2007. Comparison of disinfection byproduct formation from chlorine and alternative disinfectants. Water Res. 41 (8), 1667–1678.

Huang, H., Wu, Q.Y., Hu, H.Y., Mitch, W.A., 2012. Dichloroacetonitrile and dichloroacetamide can form independently during chlorination and chloramination of drinking waters, model organic matters, and wastewater effluents. Environ. Sci. Technol. 46 (19), 10624–10631.

Jacangelo, J.G., Trussell, R.R., 2002. International report: water and wastewater disinfection - trends, issues and practices. Water Supply 2 (3), 147–157.

Krasner, S.W., McGuire, M.J., Jacangelo, J.G., Patania, N.L., Reagan, K.M., Aieta, E.M., 1989. The occurrence of disinfection by-products in US drinking water. J. AWWA 81 (8), 41–53.

Krasner, S.W., Weinberg, H.S., Richardson, S.D., Pastor, S.J., Chinn, R., Sclimenti, M.J., et al., 2006. Occurrence of a new generation of disinfection byproducts. Environ. Sci. Technol. 40 (23), 7175–7185.

Lee, J., Giordano, S., Zhang, J., 2011a. Autophagy, mitochondria and oxidative stress: cross-talk and redox signalling. Biochem. J. 441 (2), 523–540.

Lee, W.H., Wahman, D.G., Bishop, P.L., Pressman, J.G., 2011b. Free chlorine and monochloramine application to nitrifying biofilm: comparison of biofilm penetration, activity, and viability. Environ. Sci. Technol. 45 (4), 1412–1419.

Lin, D., Bohui, X., Fanfang, Z., Prasad, S.R., 2021. Effects of nitrate and glucose on the formation of chloronitromethane (CNM) under UV/chlorine treatment. J. Water Reuse Desal. 11 (3), 475–489.

Liu, J., Zhang, X., 2014. Comparative toxicity of new halophenolic DBPs in chlorinated saline wastewater effluents against a marine alga: halophenolic DBPs are generally more toxic than haloaliphatic ones. Water Res. 65, 64–72.

Luo, T., Yu, Q., Zou, H., Zhao, H., Gu, J., Yuan, Y., et al., 2020. Role of poly (ADP-ribose) polymerase-1 in cadmium-induced cellular DNA damage and cell cycle arrest in rat renal tubular epithelial cell line NRK-52E. Environ. Pollut. 261, 114149.

Muellner, M.G., Wagner, E.D., McCalla, K., Richardson, S.D., Woo, Y.T., Plewa, M.J., 2007. Haloacetonitriles vs. regulated haloacetic acids: are nitrogen-containing DBPs more toxic? Environ. Sci. Technol. 41 (2), 645–651.

Nixdorff, H., Noga, J., Amsalu, D., Springett, J., Ashbolt, N., 2021. Improving the implementation of water and resource recovery in Canada. J. Water Reuse Desal. 11 (3), 453–463.

Nobukawa, T., Sanukida, S., 2000. The genotoxity of by-products by chlorination and ozonation of the river water in the presence of bromide ions. Water Sci. Technol. 42 (3–4), 259–264.

Peng, J., Huang, H., Zhong, Y., Yin, R., Wu, Q., Shang, C., et al., 2022. Transformation of dissolved organic matter during biological wastewater treatment and relationships with the formation of nitrogenous disinfection byproducts. Water Res. 222, 118870.

Richardson, S.D., Fasano, F., Ellington, J.J., Crumley, F.G., Buettner, K.M., Evans, J.J., et al., 2008. Occurrence and mammalian cell toxicity of iodinated disinfection byproducts in drinking water. Environ. Sci. Technol. 42 (22), 8330–8338.

Schreiber, I.M., Mitch, W.A., 2006. Nitrosamine formation pathway revisited: the importance of chloramine speciation and dissolved oxygen. Environ. Sci. Technol. 40 (19), 6007–6014.
Shackelford, R.E., Kaufmann, W.K., Paules, R.S., 1999. Cell cycle control, checkpoint mechanisms, and genotoxic stress. Environ. Health Perspect. 107, 5–24.
Shah, A.D., Mitch, W.A., 2012. Halonitroalkanes, halonitriles, haloamides, and n-nitrosamines: a critical review of nitrogenous disinfection byproduct formation pathways. Environ. Sci. Technol. 46 (1), 119–131.
Sun, D., Lin, X., Lu, Z., Huang, J., Li, G., Xu, J., 2022. Process evaluation of urban river replenished with reclaimed water from a wastewater treatment plant based on the risk of algal bloom and comprehensive acute toxicity. Water Reuse 12 (1), 1–10.
Tian, D., Moe, B., Huang, G., Jiang, P., Ling, Z.C., Li, X.F., 2020. Cytotoxicity of halogenated tyrosyl compounds, an emerging class of disinfection byproducts. Chem. Res. Toxicol. 33 (4), 1028–1035.
Turrens, J.F., 2003. Mitochondrial formation of reactive oxygen species. J. Physiol. 552 (2), 335–344.
Van der Paal, J., Neyts, E.C., Verlackt, C.C.W., Bogaerts, A., 2016. Effect of lipid peroxidation on membrane permeability of cancer and normal cells subjected to oxidative stress. Chemical Science 7 (1), 489–498.
Wang, C., Yuan, Z.X., Liu, Y.Y., Wu, Q.Y., Sun, Y.X., 2021a. Relative developmental toxicities of reclaimed water to zebrafish embryos and the relationship with relevant water quality parameters. Water Cycle 2, 85–90.
Wang, W.L., Lee, M.Y., Du, Y., Zhou, T.H., Yang, Z.W., Wu, Q.Y., et al., 2021b. Understanding the influence of pre-ozonation on the formation of disinfection byproducts and cytotoxicity during post-chlorination of natural organic matter: UV absorbance and electron-donating-moiety of molecular weight fractions. Environ. Int. 157, 106793.
Wu, Q.Y., Zhou, Y.T., Li, W., Zhang, X., Du, Y., Hu, H.Y., 2019. Underestimated risk from ozonation of wastewater containing bromide: both organic byproducts and bromate contributed to the toxicity increase. Water Res. 162, 43–52.
Xu, J., Wei, D., Wang, F., Bai, C., Du, Y., 2020. Bioassay: a useful tool for evaluating reclaimed water safety. J. Environ. Sci. 88, 165–176.
Yang, M., Zhang, X., 2013. Comparative developmental toxicity of new aromatic halogenated dbps in a chlorinated saline sewage effluent to the marine polychaete platynereis dumerilii. Environ. Sci. Technol. 47 (19), 10868–10876.
Yang, T., Wu, S., Liu, C., Liu, Y., Zhang, H., Cheng, H., et al., 2021. Efficient degradation of organoarsenic by UV/chlorine treatment: kinetics, mechanism, enhanced arsenic removal, and cytotoxicity. Environ. Sci. Technol. 55 (3), 2037–2047.
Yang, X., Fan, C., Shang, C., Zhao, Q., 2010. Nitrogenous disinfection byproducts formation and nitrogen origin exploration during chloramination of nitrogenous organic compounds. Water Res. 44 (9), 2691–2702.
Zhang, X.Y., Lu, Y., Du, Y., Wang, W.L., Yang, L.L., Wu, Q.Y., 2021a. Comprehensive GC×GC-qMS with a mass-to-charge ratio difference extraction method to identify new brominated byproducts during ozonation and their toxicity assessment. J. Hazard. Mater. 403, 124103.
Zhang, Z., Peng, Y., Zheng, J., 2021b. Amino acid and biogenic amine adductions derived from reactive metabolites. Curr. Drug Metab. 22 (14), 1076–1086.
Zheng, X.N., Wu, D.X., Huang, C.Q., Wu, Q.Y., Guan, Y.T., 2022. Impacts of hydraulic retention time and inflow water quality on algal growth in a shallow lake supplied with reclaimed water. Water Cycle 3, 71–78.